Nonlinear Absorption and Nonlinear Refraction of Self-Assembled Porphyrins

Zhi-Bo Liu,[†] Yi-Zhou Zhu,[‡] Yan Zhu,[‡] Shu-Qi Chen,[†] Jian-Yu Zheng,[‡] and Jian-Guo Tian*,[†]

The Key Laboratory of Advanced Technique and Fabrication for Weak-Light Nonlinear Photonics Materials, Ministry of Education and TEDA Applied Physical School, Nankai University, Tianjin 300457, China, and State Key Laboratory of Elemento-Organic Chemistry, College of Chemistry, Nankai University, Tianjin, 300071, China

Received: March 23, 2006; In Final Form: June 7, 2006

Nonlinear refraction and nonlinear absorption of self-assembled porphyrins in the nanosecond and picosecond regimes were studied at 532 nm by the Z-scan technique. First, a marked difference in nonlinear refraction was observed between self-assembled zinc porphyrins and free base porphyrins; however, the effects of self-assembly and metallization on nonlinear absorption are small. Second, an enhancement of nonlinear absorption was observed for the monomeric components of self-assembled structures by adding pyridine, while their nonlinear refractions remained almost unchanged as pyridine was added. It is expected that the metallization and addition of ligand can provide more convenient routes to alter the optical nonlinearities of porphyrins than the modifications of molecular structures of traditional covalent-bond organic materials.

Introduction

Organic compounds and organometallic complexes with π-electron delocalization have received significant attention in the last two decades because of their large and fast nonlinear optical response and potential applications in optical communication, data processing, optical switching, and so forth.[1,2] Porphyrins are promising candidates for such nonlinear optical (NLO) materials in view of not only large π-conjugated systems but also versatile modifications of structures and various possibilities of the central metal ion.[3,4] Most reports about optical nonlinearities of porphyrins, up to now, have been focused on reverse saturable absorption (RSA) between Soret and Q absorption bands,[5−15] off-resonant third-order nonlinearities, and two-photon absorption (TPA).[16−27] For example, under off-resonant conditions, a linear porphyrins array linked by butadiyne has been shown to exhibit among the largest $\chi^{(3)}$ values in any organic materials.[17] Anderson et al.[12] reported triply linked porphyrin with the extended region of RSA from the visible to near-infrared range. Recently, a large number of porphyrins with different molecular structures were reported on their RSA,[13−15] off-resonant third-order nonlinearities, and TPA.[21−26] However, the reports on nonlinear refraction of porphyrins in the region of RSA are few.

With the development of porphyrins,[28] a supramolecular porphyrins system with large third-order optical nonlinearities and strong TPA has been obtained by using the complementary coordination of imidazolyl to the zinc of imidazolylporphyrinatozinc(II) in the noncoordinating solvent chloroform.[19,20] The self-assembly of porphyrins greatly enhanced the off-resonant third-order nonlinearities and TPA for per-porphyrin unit. In the region of RSA, to our knowledge, the effects of self-assembly and ligand on optical nonlinearities of supramolecular porphyrins are not reported yet.

In this paper, we studied both nonlinear refraction and nonlinear absorption of self-assembled porphyrins by using a Z-scan method[29] at 532 nm in nanosecond and picosecond regimes. Compared with free base porphyrins, self-assembled zinc porphyrins have a marked difference of nonlinear refraction and but little difference of nonlinear absorption. Furthermore, the effects of the coordination solvent pyridine on optical nonlinearities of self-assembled zinc porphyrins were also observed. An enhancement of RSA was obtained by the addition of pyridine. However, the addition of pyridine cannot affect the nonlinear refraction of zinc porphyrins. We used a five-level model to simulate experimental data.

Experimental Section

Materials. Molecular structures of porphyrins studied in this work are shown in Scheme 1. Since zinc porphyrins appended with nitrogen ligands can interact with each other to form complementary dimers or multi-composites, porphyrins **1b** and **2b** to which 2-imidazolyl groups are directly attached were self-assembled to afford complementary dimers **3** and **4**.[19] Since the coordination bond can be cleaved in coordinating solvent, self-assembled porphyrin dimers can be dissociated to monomers by the addition of pyridine, and porphyrin monomers **5** and **6** can be obtained.[28]

Measurements. Electronic absorption spectra were recorded on a UV spectrophotometer (Cary 300). Nonlinear refraction and reverse saturable absorption were measured by using the closed- and open-aperture Z-scan.[29] A Q-switched Nd:YAG laser (Continuum Surelite-II) and a mode-locked Nd:YAG laser (Continuum model PY61) were used to generate 5-ns pulses and 30-ps pulses with a repetition rate of 10 Hz at 532 nm, respectively. The spatial profiles of optical pulses were nearly Gaussian obtained by spatial filtering. The beam waist was 18 μm and 20 μm for 5-ns pulses and 30-ps pulses, respectively. The incident and transmitted pulse energies were measured simultaneously with two energy detectors (Molectron J3S-10). At every position, an average of 50 incident pulses which are not beyond ±5% fluctuation was taken by a computer. The sample solutions poured in a 1-mm quartz cuvette were used with the same concentration of 2×10^{-4} mol/L. The on-axis

* Author to whom correspondence should be addressed. E-mail: jjtian@nankai.edu.cn.
[†] TEDA Applied Physical School, Nankai University.
[‡] College of Chemistry, Nankai University.

10.1021/jp061799p CCC: $33.50
Published on Web 07/14/2006

SCHEME 1: Molecular Structures of Porphyrins Studied in This Work

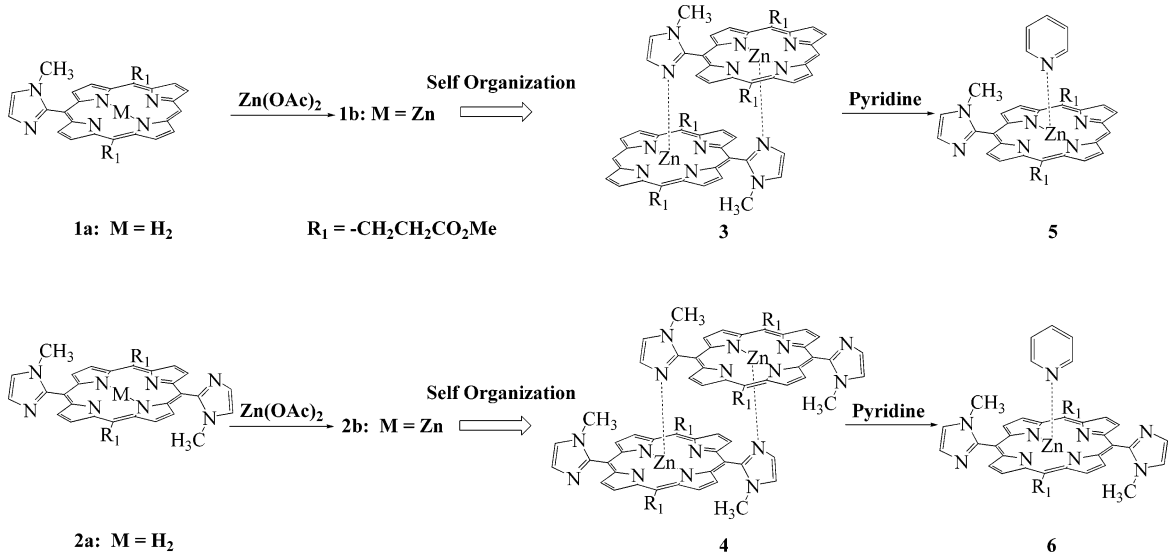

peak intensity at focus is 1.12×10^9 W/cm^2 for 5-ns pulses and 4.11×10^9 W/cm^2 for 30-ps pulses.

Synthesis of Self-Assembled Porphyrins. In a 1000-mL four-neck round-bottom flask, 0.94 g (4 mmol) of 5-(2-methoxycarbonyl-ethyl) dipyrromethane was dissolved in 600 mL of chloroform, bubbled with nitrogen for 15 min. To this solution, the mixture of 0.24 g (2.1 mmol) of 1-methyl-2-imidazolecarboxyaldehyde, 0.8 g (7 mmol) of trifluoroacetic acid in 100 mL of chloroform and 0.16 g (37%, 2 mmol) of formaldehyde, 0.92 g (20 mmol) of ethyl alcohol in 100 mL of chloroform were added simultaneously in 15 min at 40 °C. The resulting solution was stirred for 30 min, then 1.8 g (8 mmol) of DDQ was added. The mixture was passed through an aluminum oxide column after 1 h. Further purification was carried out on a silica gel column. The second red band was collected to afford **1a** 5-(1-methyl-2-imidazolyl)-10,20-bis(2-methoxy-carbonyl-ethyl)porphyrin (yield: 5%). The compound **1a** was treated with a saturated zinc acetate/methanol solution to give porphyrin zinc complex **3**. **1a** ^{1}H NMR (300 MHz, $CDCl_3$) δ 10.151 (s, 1H), 9.567 (d, $J = 4.8$ Hz, 2H), 9.517 (d, $J = 4.8$ Hz, 2H), 9.393 (d, $J = 4.8$ Hz, 2H), 8.849 (d, $J = 4.8$ Hz, 2H), 7.697 (d, $J = 1.2$ Hz, 1H), 7.491 (d, $J = 1.2$ Hz, 1H), 5.345 (t, $J = 8.1$ Hz, 4H), 3.748 (s, 6H), 3.517 (t, $J = 8.1$ Hz, 4H), 3.382 (s, 3H), −2.970 (s, 2H). FT-IR (KBr) υ 3283, 3104, 2987, 2948, 2836, 1733, 1561, 1466, 1434, 1405, 1339, 1308, 1278, 1246, 1224, 1145, 956, 919, 851, 796, 731. ESI-MS *m/z* 563 $[M + H]^+$, 1125 $[2M + H]^+$. **3** ESI-MS *m/z* 625 $[M + H]^+$, 1249 $[2M + H]^+$.

The third red band collected was proved to be **2a** 5,15-bis(1-methyl-2-imidazolyl)-10,20-bis(2-methoxycarbonyl-ethyl)porphyrin (yield: 5%). The zinc complex **4** was gained by treating **2a** with a saturated zinc acetate/methanol solution. **2a** ^{1}H NMR (300 MHz, $CDCl_3$) δ 9.532 (d, $J = 5.1$ Hz, 4H), 8.878 (m, 4H), 7.716 (m, 2H), 7.519 (m, 2H), 5.360 (t, $J = 8.4$ Hz, 4H), 3.770 (s, 6H), 3.527 (m, 10H), −2.780 (s, 2H). FT-IR (KBr) υ 3304, 3187, 3131, 3109, 2989, 2946, 2838, 1732, 1632, 1561, 1473, 1440, 1403, 1347, 1280, 1250, 1192, 1142, 1040, 980, 805, 734, 708. ESI-MS *m/z* 643 $[M + H]^+$, 1285 $[2M + H]^+$. **4** ESI-MS *m/z* 705 $[M + H]^+$, 1409 $[2M + H]^+$.

Results and Discussions

Absorption Measurements. The absorption spectra of **1a**, **2a**, **3**, and **4** shown in Figure 1a present the characteristic bands of porphyrins. The Soret bands of **1a** and **2a** are located around 411 and 417 nm, respectively. In the dimers of **3** and **4**, two porphyrins take a slipped co-facial form, and excitonic coupling between two porphyrin chromophores characteristically splits the Soret band. The Soret bands were split into twin peaks at 407 and 430 nm for **3** and at 411 and 436 nm for **4** due to exciton interaction originating from a slipped co-facial arrangement.[30] Additionally, the Soret bands of both free base and self-assembled zinc porphyrin with two imidazolyls (**2a** and **4**) have a red-shift compared with those with one imidazolyl (**1a** and **3**).

The degree of dissociation of dimers **3** and **4** depends on the amount of pyridine added. The split Soret bands of the $CHCl_3$ solution of dimers **3** and **4** can gradually turn into a single peak

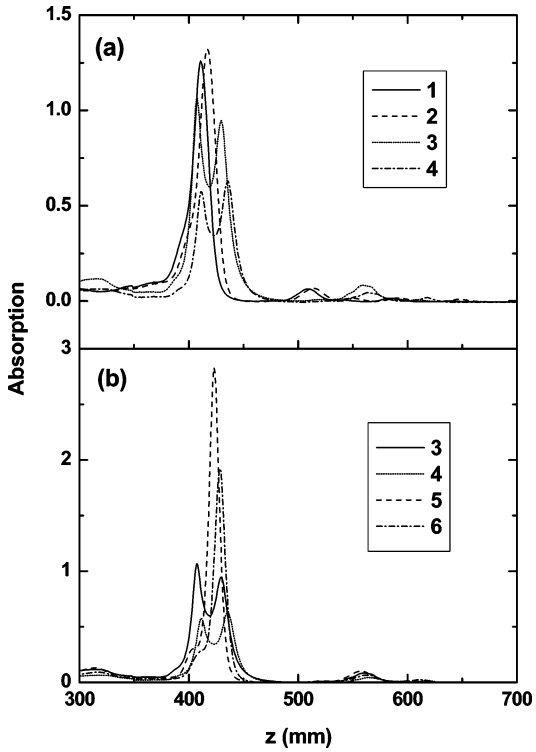

Figure 1. (a) UV absorption spectra of free base porphyrins (**1a** and **2a**) and self-assembled zinc porphyrins (**3** and **4**); (b) UV absorption spectra of **3**, **4**, **5**, and **6**.

TABLE 1: Linear and Nonlinear Optical Properties of 1a, 2a, 3, 4, 5, 6, 7 (TPP), 8 (ZnTPP), and 9 (ZnTPP−pyridine)

				picosecond pulses			nanosecond pulses		
	Soret band λ_{max} (nm)	Q−band λ^{max} (nm)	σ_0 (10^{-17} cm^2)	σ_1 (10^{-17} cm^2)	σ_{r_1} (10^{-17} cm^2)	τ_0 (ns)	σ_2 (10^{-17} cm^2)	σ_{r_2} (10^{-17} cm^2)	τ_{ISC} (ns)
1a	411	509, 584	1.24	4.1	−2.2	0.15	2.6	−1.8	8.0
2a	417	514, 590	1.62	4.5	−2.1	0.15	3.2	−1.8	6.0
3	407, 430	559, 609	1.32	3.0		0.25	1.9	−1.1	2.5
4	411, 435	564, 618	1.55	3.1		0.25	2.7	−1.1	2.0
5	423	557, 601	1.57	6.1		0.55	3.6	−1.0	1.7
6	428	562, 611	1.65	5.6		0.64	4.3	−1.1	1.5
7	418	514, 548	1.75	5.8	−1.6	0.30	4.8	−1.2	10.0
8	419	547, 584	2.65	4.2		0.45	3.5	−0.8	3.0
9	429	563, 602	2.45	4.1		0.85	2.9	−0.9	1.5

along with the addition of pyridine. When the volume ratio of pyridine to $CHCl_3$ is larger than 1:4, the change of absorption bands is so small that we can consider that the dimers **3** and **4** were completely dissociated to monomers **5** and **6**. In our experiments, we used volume 1:1 mixture solvent of pyridine and $CHCl_3$. For the monomeric imidazolylporphyrinatozinc **5** and **6**, a single peak in the Soret bands is observed as shown in Figure 1b. We can see from Figure 1 that the Q-bands of porphyrins studied in this work cover the region from 500 to 650 nm. Therefore, the laser at 532 nm used in the experiments just excites Q-bands. At this wavelength, the ground-state absorption cross-sections σ_0 of all porphyrins are shown in Table 1. As we will discuss later, a difference of optical nonlinearities between them is also observed when pyridine is added.

Effects of Metallization on Optical Nonlinearities. A large third-order optical nonlinearity of this self-assembled porphyrin system under the one-photon off-resonant condition has been observed by using femtosecond pulses.[19,20] Our work presented here involves the excited-state optical nonlinearities of self-assembled porphyrin between Soret and Q absorption bands. Through Z-scan measurements using a picosecond pulsed laser, we can obtain both the absorption and refraction cross-sections of the singlet excited state. However, we cannot determine the triplet absorption and refraction cross-sections since the triplet state cannot become populated within the picosecond pulse duration because an intersystem crossing from the second excited singlet state to the first excited triplet state is typically on the order of a nanosecond for the materials used in our experiments. Hence, to study the triplet-state absorption and refraction, a nanosecond pulsed laser has to be used. The photophysical parameters of **1a**, **2a**, **3**, and **4** measured in our experiments are summarized in Table 1.

For a nanosecond pulsed laser, a five-level model, as shown in Figure 2, can depict the excited-state absorption (ESA) process in porphyrins and other dyes. Generally, after the initial excitation of this five-level system the first excited singlet state S_1 is populated. From this state the electrons may be subsequently excited into S_2 within the pulse duration of the laser. Once arriving at S_2, they will rapidly relax to S_1 again. From

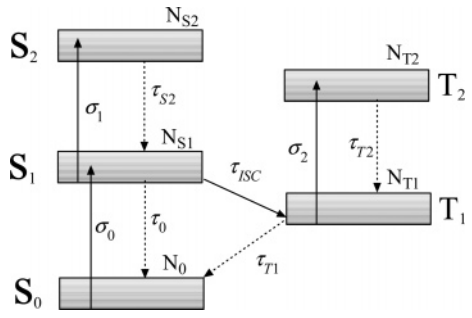

Figure 2. Five-level model of excited-state optical nonlinearities.

S_1, the population can also undergo an intersystem crossing to the first excited triplet state T_1 with a time constant τ_{ISC} and thereafter be excited into T_2. Similar to S_2, this state relaxes to T_1 rapidly. An efficient RSA material whose transmission decreases as the incident intensity increases should have a high ratio (>1) of the absorption cross-sections of the excited states σ_1 and σ_2 ($T_1 \rightarrow T_2$ and $S_1 \rightarrow S_2$) to the ground state σ_0 ($S_0 \rightarrow S_1$). Rate equations of the five-level model can be written as[31]

$$\frac{dN_{S_0}}{dt} = -\frac{\sigma_0 I N_{S_0}}{\hbar\omega} + \frac{N_{S_1}}{\tau_0} + \frac{N_{T_1}}{\tau_{T_1}} \tag{1a}$$

$$\frac{dN_{S_1}}{dt} = -\frac{\sigma_1 I N_{S_1}}{\hbar\omega} + \frac{\sigma_0 I N_{S_0}}{\hbar\omega} - \frac{N_{S_1}}{\tau_0} - \frac{N_{S_1}}{\tau_{ISC}} + \frac{N_{S_2}}{\tau_{S_2}} \tag{1b}$$

$$\frac{dN_{S_2}}{dt} = \frac{\sigma_1 I N_{S_1}}{\hbar\omega} - \frac{N_{S_2}}{\tau_{S_2}} \tag{1c}$$

$$\frac{dN_{T_1}}{dt} = -\frac{\sigma_2 I N_{T_1}}{\hbar\omega} + \frac{N_{S_1}}{\tau_{ISC}} - \frac{N_{T_1}}{\tau_{T_1}} \tag{1d}$$

$$\frac{dN_{T_2}}{dt} = \frac{\sigma_2 I N_{T_1}}{\hbar\omega} - \frac{N_{T_1}}{\tau_{T_1}} \tag{1e}$$

where N_i represents the population in the i state ($I = S_0, S_1, S_2, T_1, T_2$), I is input laser intensity, and τ_0 is the time constant of the population's transition from S_1 to S_0. If the sample length L is less than z_0, the equations that govern the irradiance and the phase change can be written as[32]

$$\frac{dI}{dz} = -\alpha I = -(\sigma_0 N_{S_0} + \sigma_1 N_{S_1} + \sigma_2 N_{T_1}) I \tag{2a}$$

$$\frac{d\phi}{dz} = k\Delta n = \sigma_{r_1} N_{S_1} + \sigma_{r_2} N_{T_1} \tag{2b}$$

where $k = 2\pi/\lambda$ is the wave vector, λ is the laser wavelength, and σ_{r_1} and σ_{r_2} are the singlet and triplet excited-state refractive cross-sections, respectively.

If the picosecond pulsed laser is used, the five-level model (S_0, S_1, S_2, T_1, and T_2) can be simplified into a three-level model (S_0, S_1, and S_2) since the intersystem crossing time τ_{ISC} is about the order of a few nanoseconds and is much larger than the pulse duration τ_p. It is difficult to obtain analytical solutions of these time- and space-dependent differential equations. Here we used the standard Runge−Kutte fourth-order method to solve eqs 1,2 numerically, and the irradiance and phase change of the laser beam at the exit face of the sample can be obtained. Then, by applying Huygens's principle and a zeroth-order

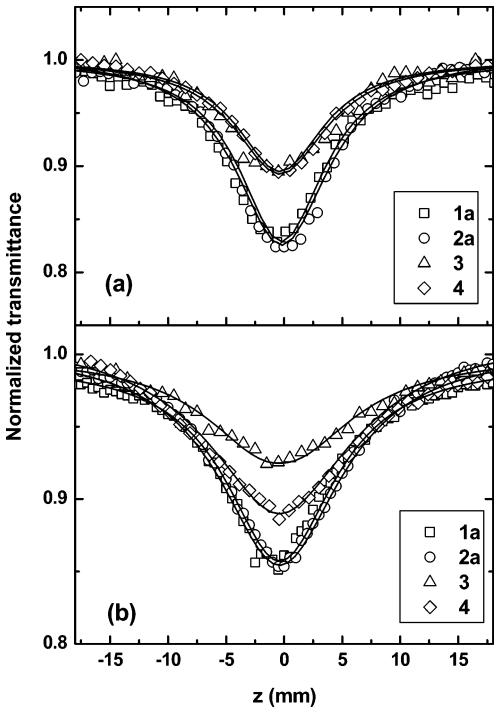

Figure 3. Open-aperture Z-scan curves of **1a**, **2a**, **3**, and **4** for the cases of picosecond pulses (a) and nanosecond pulses (b). The solid lines are the fittings obtained by a five-level model.

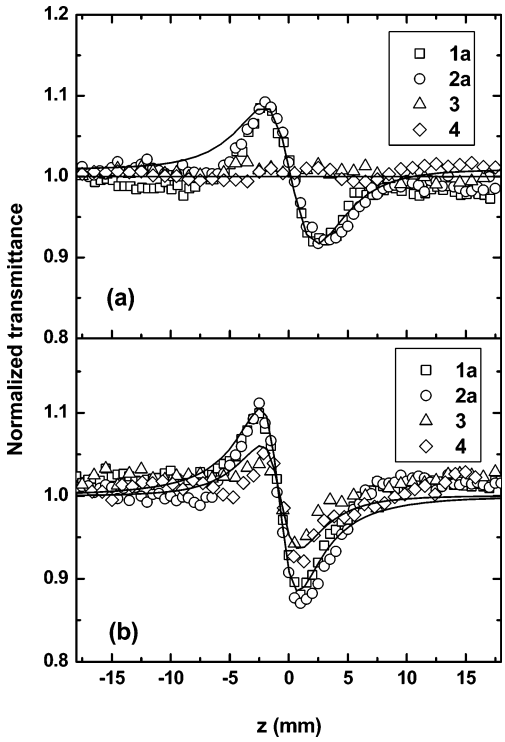

Figure 4. Nonlinear refraction Z-scan curves of **1a**, **2a**, **3**, and **4** in $CHCl_3$ for the cases of picosecond pulses (a) and nanosecond pulses (b). The solid lines are obtained by using equations (2).

Hankel transformation, we can obtain the far-field electric field at the aperture plane and the Z-scan curves. By theoretically simulating the open- and closed-aperture Z-scan experimental data, we can obtaine the values of σ_1, σ_{r_1}, and τ_0 in the case of 30-ps pulses, and σ_2, σ_{r_2}, and τ_{ISC} in the case of 5-ns pulses.[10]

The RSA properties of free base and zinc porphyrins (**1a**, **2a**, **3**, and **4**) dissolved in $CHCl_3$ are shown in Figure 3a (with 30-ps pulse duration) and Figure 3b (with 5-ns pulse duration), where open-aperture Z-scan curves were measured. The solid lines are the theoretical fittings obtained by using a five-level model. There is no obvious difference in the open-aperture Z-scan curves of **1a** and **2a** for both picosecond and nanosecond pulses. This implies that the influence of the imidazolyl is weak for free base porphyrin. It can also be seen clearly in Figure 3 that the metallization of the zinc atom results in a decrease of RSA in the cases of picosecond pulses and nanosecond pulses. This indicates that the metallization affects the absorption of both singlet and triplet excited states, since the RSA is dominated by absorption of singlet excited states in the case of picosecond pulses and by absorption of triplet excited states in the case of nanosecond pulses. For the self-assembled zinc porphyrins with one imidazolyl **3** and two imidazolyls **4**, their characteristics of RSA are similar in the case of picosecond pulses. However, **4** has a larger RSA than **3** in the case of nanosecond pulses. The difference of RSA between **3** and **4** in the case of nanosecond pulses may be due to the influence of imidazolyl on the absorption cross-section of T_1.

In the region between Soret and Q-bands, such as at 532 nm, most reports on porphyrins were concentrated on studies of RSA, but their properties of nonlinear refraction are seldom reported so far. We studied the nonlinear refraction of self-assembled porphyrins in the RSA region. Figure 4 gives the nonlinear refraction Z-scan curves of **1a**, **2a**, **3**, and **4** obtained by dividing closed-aperture Z-scan data by corresponding open-aperture Z-scan data. The solid lines are the theoretical fittings by eq 3, and the relative parameters of σ_{r_1} and σ_{r_2} are given in Table 1. For free base or self-assembled zinc porphyrins, the effect of imidazolyl on nonlinear refraction is too small to cause an observable change of nonlinear refraction Z-scan curves as shown in Figure 4. In the case of picosecond pulses, the contribution of the singlet excited state to nonlinear refraction is dominant, and using eq 3 to numerically fit the data of Figure 4a then yields $\sigma_{r_1} = -2.2 \times 10^{-17}$ cm^2 for **1a** and $\sigma_{r_1} = -2.1 \times 10^{-17}$ cm^2 for **2a**. No obvious nonlinear refraction was observed in the solution of self-assembled zinc porphyrins **3** and **4**, and this implies that the nonlinear refraction arising from the singlet excited state is very small. To our knowledge, it is the first time that the disappearance of nonlinear refraction was observed through the metallization at 532 nm.

To determine the nonlinear refractive cross-section of the triplet excited state σ_{r_2}, we performed closed-aperture Z-scans using a nanosecond pulsed laser and fitted the experimental data, as shown in Figure 4b. This yielded a σ_{r_2} of -1.8×10^{-17} cm^2 for free base porphyrins (**1a** and **2a**) and -1.1×10^{-17} cm^2 for self-assembled zinc porphyrins (**3** and **4**). The metallization of the zinc atom also caused a decrease of nonlinear refraction like its effect on RSA. However, it can be seen from Table 1 that the decrease of σ_{r_2} due to the metallization is smaller than that of σ_{r_1}, indicating that the effect of metallization on **the** singlet excited state is larger than that on the triplet excited state. In the case of nanosecond pulses, the thermal effect should be generally taken into account for the measurements of nonlinear refraction. The thermal effect arises from acoustic wave propagation caused by medium density change after local heating, and its buildup time is determined by the time required for a sound wave to propagate across beam size, $\tau_{ac} = \omega_0/c_S$, where c_S is the velocity of sound in the medium. In our experimental condition, the value of τ_{ac} ($\approx$20 ns) is much larger than the duration of pulses $\tau_p = 5$ ns. Therefore, the thermal effect can be neglected when the nanosecond pulsed laser is used.[33,34]

For self-assembled zinc porphyrins such as **4**, Yoshiaki Kobuke et al.[19,20,27] have employed the femtosecond time-

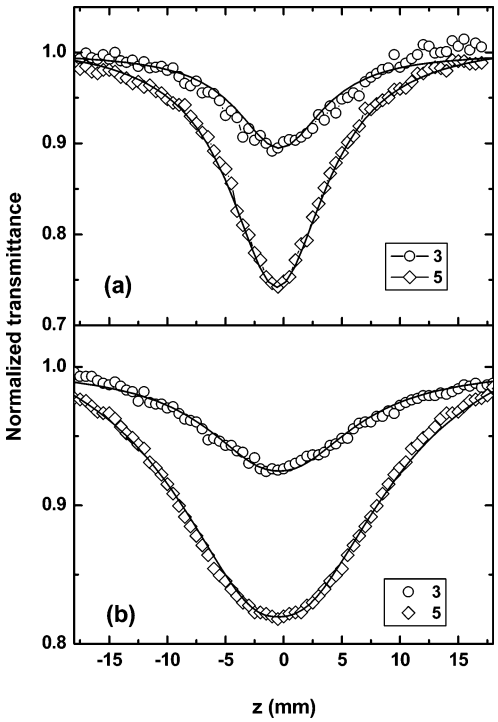

Figure 5. Open-aperture Z-scan curves of **3** and **5** in the cases of picosecond pulses (a) and nanosecond pulses (b).

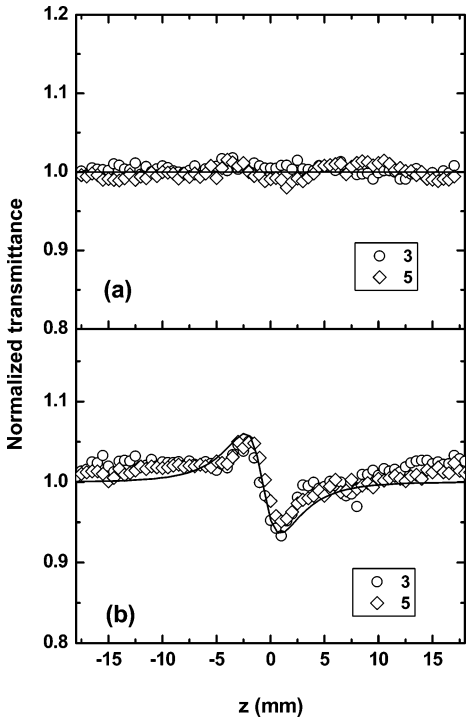

Figure 6. Nonlinear refraction Z-scan curves of **3** and **5** in the cases of picosecond pulses (a) and nanosecond pulses (b).

resolved optical Kerr effect and Z-scan methods to measure the third-order optical nonlinearities in the off-resonance condition. The optical nonlinearities from electronic polarization in the off-resonance condition, which involves the distortion of the electron cloud about an atom or molecule by the optical field, was obtained and the susceptibility $|\chi_{yyyy}^{(3)}|$ is 2.4×10^{-14} esu at 800 nm with a concentration of 1.5×10^{-4} M.

Effect of Ligand on Optical Nonlinearities. In our experiments, the coordination solvent pyridine was added in the $CHCl_3$ solutions of self-assembled zinc porphyrin. Since the coordination bond can be cleaved by adding a coordinating solvent, the dimers **3** and **4** were dissociated to monomers **5** and **6** with the addition of pyridine, which leads to a transition of Soret bands from the split band into a single peak, as shown in Figure 1b. Besides the induced change of linear absorption, the addition of coordination solvent can also result in a change of RSA for self-assembled zinc porphyrins. Figure 6 gives the open-aperture Z-scan curves of **3** and **5** in the cases of picosecond pulses (part a) and nanosecond pulses (part b), respectively. The results are summarized in Table 1. The values of excited-state absorption cross-sections are raised to 6.1×10^{-17} from 3.0×10^{-17} cm^2 for σ_1 and to 3.4×10^{-17} from 1.9×10^{-17} cm^2 for σ_2, respectively, when pyridine was added in porphyrins **3**. For zinc porphyrins **4** with two imidazolyls, an enhancement of both singlet and triplet excited-state absorption cross-sections can also be found in Table 1 when pyridine was present. Meanwhile, it can be seen from Table 1 that the change of the ground-state absorption cross-section σ_0 is small when pyridine is added. The fixity of σ_0 and the enhancement of σ_1 and σ_2 can cause the improvement of figure of merit (σ_1/σ_0 and σ_2/σ_0) that is an important parameter in the application of optical limiting.

The enhancement of RSA may arise from the significantly different symmetries between the monomers (**5** and **6**) and the assemblies (**3** and **4**). The different symmetries will cause different electronic distributions. For assemblies (**3** and **4**), the Soret band corresponding to higher singlet excited-state S_2 is nondegenerate depending on the head-to-tail and face-to-face orientations of transitions dipoles.[30] In the monomers (**5** and **6**), however, the Soret band is degenerate due to symmetry. The different electronic distributions may result in different properties of RSA between the monomers (**5** and **6**) and the assemblies (**3** and **4**). Furthermore, the cooperative assembly of the dimers results in a robust system that likely remains together as the heat is dissipated from the supramolecular compounds. Conversely, the axial coordination of pyridine by zinc porphyrins is quite weak so the pyridine probably transiently comes off the metalloporphyrins.[35]

The Z-scan experiments of **1a** and **2a** with the addition of pyridine have also been performed, and no obvious change was observed because there is no coordination interaction between free base porphyrins and pyridine.

The nonlinear refraction Z-scan curves of **3** and **5** are shown in Figure 6. Opposite to RSA, the addition of pyridine cannot result in an observable change of nonlinear refraction for both one imidazolyl and two imidazolyls porphyrins, and the values of σ_{r_1} and σ_{r_2} of **5** and **6** are shown in Table 1. This illustrates that the complementary coordination of ligands to zinc has no contribution to nonlinear refraction, but it does have a large influence on RSA in the cases of both picosecond and nanosecond pulses. For picosecond pulses, although singlet and triplet excited-state absorption cross-sections are enhanced when pyridine is added, the nonlinear refraction was still absent. Therefore, the disappearance of nonlinear refraction should be mainly caused by the metallization of zinc.

The Z-scan experiments were also carried out for simple zinc and free base tetraphenylporphyrins (ZnTPP and TPP) in $CHCl_3$. The change of nonlinear refraction is similar to that of self-assembled porphyrins, indicating that the metallization of zinc can mainly affect nonlinear refraction. However, no obvious change of RSA was obtained by adding pyridine into ZnTPP in the case of picosecond pulses.[36] In the case of nanosecond pulses, the addition of pyridine in ZnTPP resulted in a small decreasing of RSA,[36] which is different from enhancement of

RSA in the self-assembled porphyrin system. The data of TPP (**7**), ZnTPP (**8**), and ZnTPP−pyridine (**9**) are given in Table 1.

It is very interesting that the coordination of pyridine to zinc porphyrins can only affect their properties of RSA, and their nonlinear refraction cannot be obviously altered. Oppositely, the demetallization of the zinc atom at the center of porphyrin rings can mainly result in a decrease of nonlinear refraction. To realize the control of optical nonlinearities and find materials with large optical nonlinearities, more efforts have been undertaken to establish the relationship between structure and nonlinear optical response for organic molecules in order that materials in particular applications can be rationally designed and synthesized.[3,11] The ligands substitution in the supramolecular porphyrin system provides a convenient approach to alter optical nonlinearities of porphyrins. It can be realized much more easily and flexibly than modifying molecular structure of traditional covalent bond organic materials.[19,20] Furthermore, through the combination of the addition of pyridine and the metallization of the zinc atom, nonlinear refraction and RSA can be adjusted solely.

Conclusions

In summary, this work points out that metallization and coordination of solvent to zinc have large effects on nonlinear refraction and RSA for imidazolylporphyrins. In the picosecond regime, a drastic decrease of nonlinear refraction was observed in self-assembled zinc porphyrins. The change of nonlinear refraction is mainly attributed to the metallization. An enhancement of RSA was obtained by adding pyridine to self-assembled zinc porphyrins in the cases of both picosecond and nanosecond pulses. In this supramolecular system, the molecular length and the structure of the central π-conjugation system are easily modified. The flexible control of linear and nonlinear optical properties can be realized by using different noncovalent bonds. Efforts are being undertaken to further enhance and characterize optical nonlinearities of supramolecular porphyrins.

Acknowledgment. The authors acknowledge the support of the Preparatory Project of the National Key Fundamental Research Program (Grant 2004CCA04400), the Natural Science Foundation of China (Grants 10574075, 20172028, and 20421202), and the Program for Changjiang Scholars and Innovative Research Team in University.

References and Notes

(1) Prasad, P. N.; Williams, D. J. *Introduction to Nonlinear Optical Effects in Molecules and Polymers*; Wiley: New York, 1991.
(2) Nalwa, H. R.; Miyata, S. *Nonlinear Optics of Organic Molecules and Polymers*; CRC Press: Boca Raton, FL, 1997.
(3) Torre, G. D. L.; Vazquez, P.; Agullo-Lopez, F.; Torres, T. *Chem. Rev.* **2004**, *104*, 3723.
(4) Calvete, M.; Yang, G. Y.; Hanack, M. *Synth. Met.* **2004**, *141*, 231.
(5) Blau, W.; Byrne, H.; Dennis, W. M.; Kelly, J. M. *Opt. Commun.* **1985**, *56*, 25.
(6) Henari, F. Z.; Blau, W. J.; Milgram, L. R.; Yahioglu, G.; Phillips, D.; Lacey, J. A. *Chem. Phys. Lett.* **1997**, *267*, 229.
(7) Rao, S. V.; Naga Srinivas, N. K. M.; Rao, D. N.; Giribabu, L.; Maiya, B. G.; Philips, R.; Kumar, G. R. *Opt. Commun.* **2000**, *182*, 255.
(8) Ono, N.; Ito, S.; Wu, C. H.; Chen, C. H.; Wen, T. C. *Chem. Phys.* **2000**, *262*, 467.
(9) McEwan, K. J.; Bourhill, G.; Robertson, J. M.; Anderson, H. L. *J. Nonlinear Opt. Phys. Mater.* **2000**, *9*, 451.
(10) Kiran, P. P.; Reddy, D. R.; Maiya, B. G.; Dharmadhikari, A. K.; Kumar, G. R.; Desai, N. R. *Appl. Opt.* **2002**, *41*, 7631.
(11) McEwan, K.; Lewis, K.; Yang, G. Y.; Chng, L. L.; Lee, Y. W.; Lau, W. P.; Lai, K. S. *Adv. Funct. Mater.* **2003**, *13*, 863.
(12) McEwan, K.; Fleitz, P.; Rogers, J.; Slagle, J.; McLean, D.; Akdas, H.; Katterle, M.; Blake, I.; Anderson, H. *Adv. Mater.* **2004**, *16*, 1933.
(13) McKerns, M. M.; Sun, W.; Lawson, C. M. *J. Opt. Soc. Am. B* **2005**, *22*, 852.
(14) Jiang, L.; Lu, F.; Li, H.; Chang, Q.; Li, Y.; Liu, H.; Wang, S.; Song, Y.; Cui, G.; Wang, N.; He, X.; Zhu, D. *J. Phys. Chem. B* **2005**, *109*, 6311.
(15) Neto, N. M. B.; Boni, L. D.; Mendonca, C. R.; Misoguti, L.; Queiroz, S. L.; Dinelli, L. R.; Batista, A. A.; Zilio, S. C. *J. Phys. Chem. B* **2005**, *109*, 17340.
(16) Kandasamy, K.; Shetty, S. J.; Puntambekar, P. N.; Srivastava, T. S.; Kundu, T.; Singh, B. P. *J. Porphyrins Phthalocyanines* **1999**, *3*, 81.
(17) Kuebler, S. M.; Denning, R. G.; Anderson, H. L. *J. Am. Chem. Soc.* **2000**, *122*, 339.
(18) Screen, T. E.; Thorne, J. R. G.; Denning, R. G.; Bucknall, D. G.; Anderson, H. L. *J. Am. Chem. Soc.* **2002**, *124*, 9712.
(19) Ogawa, K.; Zhang, T.; Yoshihara, K.; Kobuke, Y. *J. Am. Chem. Soc.* **2002**, *124*, 22.
(20) Ogawa, K.; Ohashi, A.; Kobuke, Y.; Kamada, K.; Ohta, K. *J. Am. Chem. Soc.* **2003**, *125*, 13356.
(21) Ikeda, C.; Yoon, Z. S.; Park, M.; Inoue, H.; Kim, D.; Osuka, A. *J. Am. Chem. Soc.* **2005**, *127*, 534.
(22) Drobizhev, M.; Stepanenko, Y.; Dzenis, Y.; Karotki, A.; Rebane, A.; Taylor, P. N.; Anderson, H. L. *J. Phys. Chem. B* **2005**, *109*, 7223.
(23) Kim, D. Y.; Ahn, T. K.; Kwon, J. H.; Kim, D.; Ikeue, T.; Aratani, N.; Osuka, A.; Shigeiwa, M.; Maeda, S. *J. Phys. Chem. A* **2005**, *109*, 2996.
(24) Collini, E.; Ferrante, C.; Bozio, R. *J. Phys. Chem. B* **2005**, *109*, 2.
(25) Ahn, T. K.; Kwon, J. H.; Kim, D. Y.; Cho, D. W.; Jeong, D. H.; Kim, S. K.; Suzuki, M.; Shimizu, S.; Osuka, A.; Kim, D. *J. Am. Chem. Soc.* **2005**, *127*, 12861.
(26) Rath, H.; Sankar, J.; PrabhuRaja, V.; Chandrashekar, T. K.; Nag, A.; Goswami, D. *J. Am. Chem. Soc.* **2005**, *127*, 11608.
(27) Ogawa, K.; Ohashi, A.; Kobuke, Y.; Kamada, K.; Ohta, K. *J. Phys. Chem. B* **2005**, *109*, 22003.
(28) Satake, A.; Kobuke, Y. *Tetrahedron* **2005**, *61*, 13.
(29) Sheik-Bahae, M.; Said, A. A.; Wei, T. H.; Hagan, D. J.; Van Stryland, E. W. *IEEE J. Quantum Electron.* **1990**, *26*, 760.
(30) Kobuke, Y.; Miyaji, H. *J. Am. Chem. Soc.* **1994**, *116*, 4111.
(31) Wei, T. H.; Huang, T. H.; Wu, T. T.; Tsai, P. C.; Lin, M. S. *Chem. Phys. Lett.* **2000**, *318*, 53.
(32) Wei, T. H.; Hagan, D. J.; Sence, M. J.; Van Stryland, E. W.; Perry, J. W.; Coulter, D. R. *Appl. Phys. B* **1992**, *54*, 46.
(33) Kovsh, D. I.; Hagan, D. J.; Van Stryland, E. W. *Opt. Express* **1999**, *4*, 315.
(34) Liu, Z. B.; Zhou, W. Y.; Tian, J. G.; Chen, S. Q.; Zang, W. P.; Song, F.; Zhang, C. P. *Opt. Commun.* **2005**, *245*, 377.
(35) Retsek, J. L.; Drain, C. M.; Kirmaier, C.; Nurco, D. J.; Medforth, C. J.; Smith, K. M.; Sazanovich, I. V.; Chirvony, V. S.; Fajer, J.; Holten, D. *J. Am. Chem. Soc.* **2003**, *125*, 9787.
(36) Kimball, B. R.; Nakashima, M.; DeCristofano, B. S.; Srinivas, N. K. M. N.; Premkiran, P.; Rao, D. N.; Panchangam, A.; Rao, D. V. G. L. N. *Proc. SPIE* **2000**, *4106*, 264.